Direct observation of shear piezoelectricity in poly-l-lactic acid nanowires

Michael Smith, Yonatan Calahorra, Qingshen Jing, and Sohini Kar-Narayan

Citation: APL Materials **5**, 074105 (2017); doi: 10.1063/1.4979547
View online: http://dx.doi.org/10.1063/1.4979547
View Table of Contents: http://aip.scitation.org/toc/apm/5/7
Published by the American Institute of Physics

APL MATERIALS **5**, 074105 (2017)

Direct observation of shear piezoelectricity in poly-L-lactic acid nanowires

Michael Smith, Yonatan Calahorra, Qingshen Jing, and Sohini Kar-Narayan[a]
Department of Materials Science and Metallurgy, University of Cambridge, 27 Charles Babbage Road, Cambridge CB3 0FS, United Kingdom

(Received 2 February 2017; accepted 20 March 2017; published online 6 April 2017)

Piezoelectric polymers are capable of interconverting mechanical and electrical energy, and are therefore candidate materials for biomedical applications such as sensors, actuators, and energy harvesters. In particular, nanowires of these materials are attractive as they can be unclamped, flexible and sensitive to small vibrations. Poly-L-lactic acid (PLLA) nanowires have been investigated for their use in biological applications, but their piezoelectric properties have never been fully characterised, even though macroscopic films and fibres have been shown to exhibit shear piezoelectricity. This piezoelectric mode is particularly interesting for *in vivo* applications where shear forces are especially relevant, and is similar to what has been observed in natural materials such as bone and DNA. Here, using piezo-response force microscopy (PFM), we report the first direct observation of shear piezoelectricity in highly crystalline and oriented PLLA nanowires grown by a novel template-wetting method. Our results are validated using finite-element simulations and numerical analysis, which importantly and more generally allow for accurate interpretation of PFM signals in soft nanostructured materials. Our work opens up the possibility for the development of biocompatible and sustainable piezoelectric nanogenerators and sensors based on polymer nanowires. [http://dx.doi.org/10.1063/1.4979547]

The occurrence of piezoelectricity in biological materials is remarkably common.[1,2] Collagenous tissues such as bone, skin, and tendon,[3,4] as well as cellulose[5] and even DNA[6] have all been reported to possess piezoelectric properties. Common to all these materials is a helical conformation of the polymer chain. As a result, all these materials exhibit *shear* piezoelectricity; a coupling between a uniaxial polarisation and a shear stress or strain. One such material is poly-L-lactic acid (PLLA), which is well-known for its many remarkable properties, including the ability to exhibit piezoelectric behaviour following appropriate treatment.[7–9] PLLA is also biologically derived (typically produced from bacterial fermentation of corn starch) and biodegradable. It is therefore often proposed as a replacement for traditional oil based plastics in packaging applications,[10,11] and as resorbable tissue scaffolds in biomedicine.[12,13] The combination of piezoelectricity, biocompatibility, and sustainability makes PLLA an interesting material to investigate, especially when considering tissue engineering and biomedical sensing,[14,15] as well as *in vivo* energy harvesting applications as nanogenerators.[16,17]

There are four known crystal phases of PLLA (α', α, β, and γ); all of which are based around a helical conformation of the polymer chain (see the supplementary material, S1). A satisfactory mechanism relating the crystal structure to the piezoelectric properties of PLLA has yet to be formulated; however it is known that both crystallinity and alignment of the polymer chains are required to reveal the behaviour.[18] Oriented PLLA belongs to the D_∞ point group; therefore the non-zero components of the piezoelectric tensor are $d_{14} = -d_{25}$ (expressed using Voigt notation, with the 3 axis parallel to the direction of chain orientation). In terms of the converse piezoelectric effect, an electric field applied along the '1' direction will result in a shear strain *about* the '1' axis. A value of 10 pC/N is most often quoted for d_{14}, determined from measurements of the uniaxially drawn bulk film;[7,9]

[a]Email: sk568@cam.ac.uk

however the exact value observed will be dependent on the degree of crystallinity and alignment in the material.[19]

PLLA nanofibers are commonly produced by electrospinning,[12] but the relatively low crystallinity of electrospun nanofibers means that this is not the optimum production method for investigating the piezoelectric properties of PLLA nanostructures.[20–22] Template wetting is an alternative, versatile technique that has been widely used to produce nanostructures from a large range of polymers.[23–28] The method involves a thin membrane with through-thickness nanometer sized pores (referred to herein as the "template") being infiltrated with the polymer solution or polymer melt. Crystallisation within the confined environment of a nanopore leads to high aspect ratio nanostructures, often exhibiting preferential chain alignment and, in the case of ferroelectric polymers, some spontaneous remnant polarisation.[29,30] This can have significant implications on the material's piezoelectric properties. Here, we demonstrate for the first time, a simple and versatile template-wetting method that has been developed to produce oriented and highly crystalline nanowires of PLLA that are subsequently shown to exhibit shear piezoelectricity.

The works of Tajitsu *et al.*,[31,32] Ito *et al.*,[33] and Ando *et al.*[34] have demonstrated how shear piezoelectricity can be used to create versatile sensors and actuators from PLLA films and fibres. Creating nanostructures of a material that exhibits strong shear piezoelectricity is an interesting prospect. For a PLLA nanowire with the crystallographic 3 axes aligned along its length, an electric field applied across its diameter will cause the nanowire to *bend*. Conversely, flexing or bending of such nanowires will likely produce a larger electrical response than axial deformation in this material. The high aspect ratio and unconstrained nature of the nanostructure ought to allow this behaviour to be fully expressed, with many potential applications in energy harvesting and sensing.[16,25,35,36]

The piezoelectric properties of electrospun PLLA nanofibres have only been briefly studied. Lee *et al.*[37] investigated the piezoelectric response of an electrospun PLLA nanofiber web subject to periodic loading, using a method characteristic of energy-harvesting device testing. However, such a method does not allow for the direct observation of the *shear* piezoelectric properties of the PLLA nanofibres. The most rigorous route for characterising the piezoelectric properties of PLLA nanostructures is to observe the response from an individual specimen using piezo-response force microscopy (PFM). The proper use of the technique enables comprehensive characterisation of the piezoelectric response for a wide variety of materials with nanoscale resolution.[38,39]

PFM is often used to investigate piezoelectric nanostructures,[40,41] including polymer nanowires.[42] The vertical PFM signal corresponds to out-of-plane displacements of the material in response to an applied electric field while the lateral PFM signal corresponds to in-plane displacements. The in-plane displacement characteristic of shear piezoelectricity in bone has previously been observed using the lateral PFM signal, i.e., torsional deflection of the AFM tip along the cantilever length.[43] However, PFM studies on nanostructured PLLA are rare, with only one report of a PFM study on electrospun PLLA nanofibers,[44] though this work does not report the lateral tip deflection nor demonstrate the shear piezoelectric behaviour from the observed signals. Furthermore, a piezo-response was only obtained after the material was subjected to local poling with electric fields in excess of 10^8 V m^{-1}, even though PLLA is not a ferroelectric material and hence not expected to respond to electrical poling. In this work, we conduct rigorous PFM studies on individual PLLA nanowires with a thorough investigation of the origins of the measured PFM signals. Our studies thus reveal the first direct observation of shear piezoelectricity in PLLA nanowires using the PFM technique.

Importantly, there are two key points which must be carefully considered when analysing PFM data on piezoelectric nanowires but which are often overlooked. First, the non-planar geometry of nanowires with curvatures of the same order as that of the AFM tip apex itself needs to be considered in the analysis of PFM data. Second, the electric field between the tip and substrate is non-uniform, similar to that of a point charge. The consequences of non-planar topography and non-uniform field are addressed by Denning and Peter *et al.*,[45–47] and are also are discussed in more detail in the supplementary material, S4. In view of the above, we present detailed numerical modelling of such a system. A finite element analysis (FEA) of the PFM measurement, accounting for the issues mentioned above, was constructed to rationalise the measured PFM signals from our PLLA nanowires. The results indicate that template-grown PLLA nanowires exhibit strong shear piezoelectricity, and

more generally that FEA modelling, as presented here, is necessary to fully understand the results of PFM on piezoelectric nanowires.

Figure 1 illustrates the novel temperature-controlled capillary infiltration method used to grow the PLLA nanowires used in this study. A silver-capped anodised aluminium oxide (AAO) porous template (with nominal pore diameter 200 nm and thickness 60 μm) was floated onto heated PLLA solution (10 wt. % in 1,4-dioxane) and allowed to infiltrate via capillary action. Residual solution and the Ag capping layer were removed following infiltration, revealing PLLA nanowires contained within the AAO template. The template was then selectively etched using phosphoric acid to release the nanowires. See the supplementary material, S2, for details of nanowire fabrication. Scanning electron microscopy (SEM) images demonstrate the solid, rod-like structure and uniform morphology of the nanowires.

By varying the temperature of the PLLA solution (herein referred to as the 'infiltration temperature,' T_i), the crystallinity of the nanowires could be reliably controlled, as shown by the differential scanning calorimetry (DSC) traces in Figure 2(a). Significant cold crystallisation occurs on heating through ≈70 °C for the nanowires grown at 40 and 60 °C, suggesting that some degree of chain alignment exists within the amorphous regions of the material, but the reduced chain mobility at low infiltration temperatures prevents complete crystallisation during growth. Only as the infiltration temperature exceeds the glass transition temperature of the polymer (approximately 60 °C [10]) does chain mobility improve to facilitate greater crystallisation during growth. The crystalline fraction was determined, accounting for cold crystallisation, using a standard enthalpy of 93.6 J g^{-1} for melting of 100% crystalline PLLA.[48] A maximum crystallinity of 70% ± 5% for an infiltration temperature of 100 °C was achieved, readily reproduced, and verified by comparison with the crystallinity estimated from x-ray diffraction data.

Rigorous phase identification in PLLA via wide-angle X-ray diffraction (WAXD) in Bragg-Brentano geometry is particularly challenging, owing to the similarities between crystal structures.[49] Nonetheless, some useful structural information could still be obtained owing to one of the significant benefits of the template-wetting method, namely the physical alignment of the nanowires within the template material.

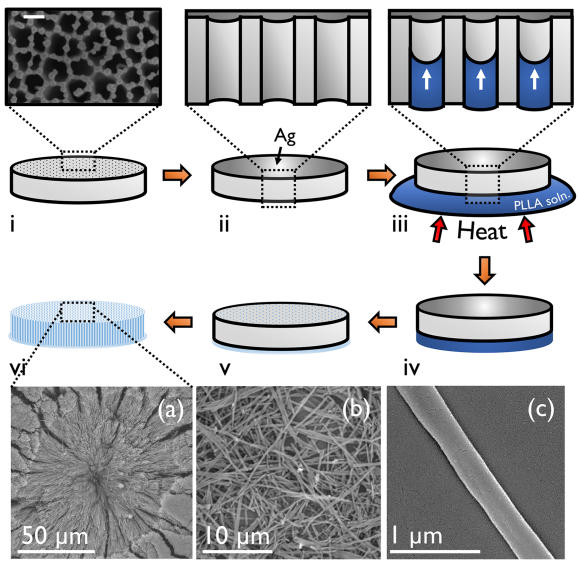

FIG. 1. A schematic of the temperature controlled capillary infiltration process used to grow the PLLA nanowires. (i) The porous AAO template (scale bar represents 200 nm). (ii) A capping layer of silver is sputtered onto the uppermost surface of the template, sealing the pores from one side. (iii) The capped template is floated onto a droplet of 10 wt. % solution of PLLA in 1,4-dioxane. The temperature of the solution is controlled using a hotplate. Capillary action causes the solution to infiltrate the nanopores. (iv) The infiltrated template is lifted from the droplet after 10 min. (v) Any residual solvent is removed. The capping silver layer is removed using ferric nitrate. (vi) The template material is selectively etched in phosphoric acid, revealing the PLLA nanowires—(a) immediately after etching, (b) collected as a nanowire "powder," (c) an individual PLLA nanowire.

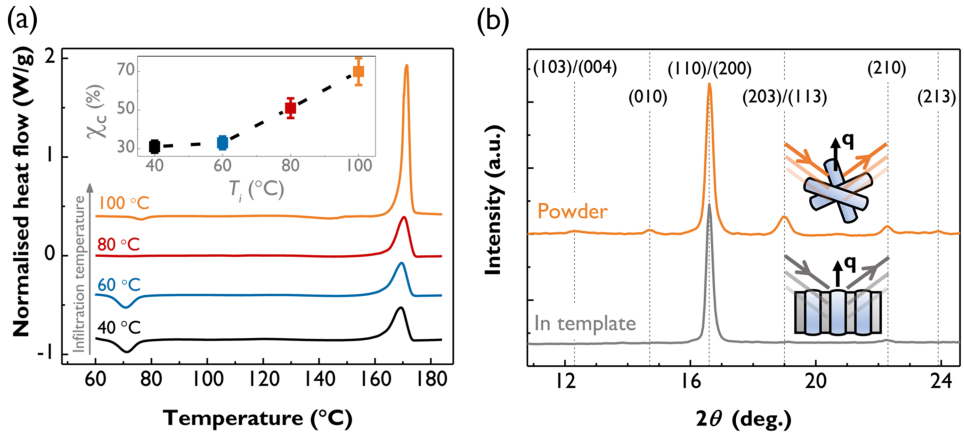

FIG. 2. (a) DSC heat flow, obtained at a heating rate of 5 °C/min. Cold crystallisation events occur for the nanowires infiltrated at lower temperatures, indicative of an aligned but non-crystalline polymer. The crystallinity (χ_c) is also shown for each infiltration temperature, reaching a maximum of 70% ± 5%. (b) XRD patterns collected from nanowires as a powder and within the template. The cartoons depict the orientation of the measured scattering vector with respect to the nanowires. The presence of more reflections in the powdered case is evidence for crystallographic alignment in the nanowires.

WAXD of the nanowires whilst held within the template could be compared to equivalent scans from a nanowire powder, thus revealing information about the alignment of polymer chains within the nanowires. This comparison is shown in Figure 2(b) for nanowires grown at an infiltration temperature of 100 °C. When characterised within the template, only one significant reflection is observed, attributed to inter-chain scattering from (110) & (200) planes, typical of many polymer systems. As a powder, many more reflections were observed, producing a pattern consistent with the α crystal phase of PLLA[49–52] (see the supplementary material, S1). In line with our XRD results, we expect that the high degree of shear force experienced by the polymer solution during capillary infiltration, especially in the vicinity of the pore walls, led to some molecular alignment of the polymer chains along the length of the nanowire.[53] At high infiltration temperatures, the chain mobility was sufficient to enable the polymer to crystallise in this aligned state, forming highly crystalline and aligned structures.

Our structural characterisation therefore demonstrates that temperature-controlled capillary infiltration allows the formation of highly crystalline and molecularly aligned nanowires of PLLA. A maximum crystallinity of ≈70% from the as-prepared nanowires found exceeds the typical 30%-40% crystalline fraction achievable with electrospun nanofibers.[20,21,54] Therefore, this production method is ideally suited to fabrication of piezoelectric PLLA nanostructures, given that both crystallinity and alignment are prerequisites for the observation of piezoelectricity in PLLA.

PFM was subsequently used to investigate the piezoelectric properties of individual nanowires, grown at an infiltration temperature of 100 °C to ensure maximum crystallinity. The scanning geometry used to acquire these signals is displayed in Figure 3(a). The fast scan direction (x) and the lateral PFM deflection (y) were intentionally kept orthogonal to minimise any coupling between the two. The topography (contact mode), lateral (y-axis), and vertical (z-axis) PFM deflections from an individual PLLA nanowire are shown in Figures 3(b)–3(d).

Significant broadening of the nanowires was observed due to tip convolution effects. The best estimate of the nanowire diameter is the measured height, which was in agreement with the dimensions of the AAO pores. Significant deflection was seen in the lateral signal across the entire (tip-broadened) effective width. Conversely, a sharp vertical response was observed only at the very edges of the nanowire. While the images shown in Figure 3 are representative, the same distinct response was observed from multiple individual nanowires.

Due to the complex interaction between the non-planar nanowire and non-uniform electric field, the interpretation of these signals is non-trivial. A finite element computational model (COMSOL Multiphysics 5.2) was used to simulate the PFM signals which would be expected from a PLLA nanowire exhibiting shear piezoelectricity, assuming alignment of the crystallographic '3' axis along the nanowire length (as expected for this growth method) and a piezoelectric coefficient $d_{14} = 10$ pC/N.

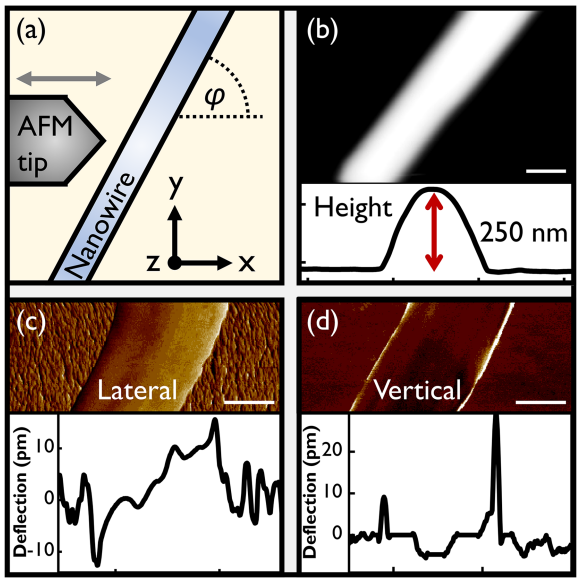

FIG. 3. (a) PFM scanning geometry. The fast scan direction is along the *x*-axis, the lateral signal is the deflection along the *y*-axis. (b) Topography of a single nanowire, approximately 250 nm in diameter. Tip convolution effects lead to a significant increase in the measured diameter. (c) Lateral and (d) vertical PFM signals from a single nanowire, acquired with a 10 V oscillating potential. Values of deflection are subject to an error of 3%. Scale bars represent 500 nm.

Details of this model can be found in S6 of the supplementary material, with animations of nanowire deformation and electric field between the tip and nanowire during scanning shown in the video files (see the supplementary material, S7).

The signal acquired from any PFM measurement has contributions not only from the piezoelectric response but also from any material electrostriction or electrostatic interaction.[38,55,56] Decoupling these effects is crucial if it is to be conclusively stated that the material in question is indeed piezoelectric. One of the characteristic features of the (converse) piezoelectric effect is a linear dependence on the applied field. In contrast, electrostrictive and electrostatic phenomena are *non*-linear in the applied field, typically displaying parabolic dependence. Demonstrating a linear response of the PLLA nanowires to the applied field is therefore required to further add to the evidence of piezoelectric activity in these nanostructures.

However, given the complexity of the system, it is not immediately obvious how a linear response will manifest itself in the measured PFM deflections. The FEA model can be used to predict the lateral PFM response as a function of applied voltage, as shown in Figure 4(a). It can be seen that the magnitudes of the peaks at ±250 nm vary linearly with the applied voltage. Moreover, the *gradient* of the deflection as measured between the two peaks (using linear regression) is also directly proportional to the applied voltage.

Figure 4(b) shows this analysis performed on lateral PFM traces obtained from the same nanowire at applied voltages of 0, 4, and 8 V (see the supplementary material, S5, for the full set of images). Whilst noisy, gradients can be readily calculated using linear regression and when plotted as a function of applied voltage display a linear relationship. Therefore, given the similarities between modelled and experimental results, we can confidently assert that the PLLA nanowires do indeed exhibit shear piezoelectricity.

In order to fully characterize the shear piezoelectric behaviour of these nanowires, it is desirable to obtain a value of d_{14}, which in principle can be determined through comparison of the measured and simulated deflection gradients. Comparing the measured voltage sensitivity from the PLLA nanowires (the gradient of the line in Figure 4(b–ii), 8.9×10^{-7} V^{-1}) to a calibration line generated from computer modelling, d_{14} can be estimated as ≈ 8 pC/N (see the supplementary material, S8, for details of this estimate). While there is room for improvement in the estimation of the model parameters, our estimated value of d_{14} for template-grown PLLA nanowires was found to be consistent with the often quoted 10 pC/N bulk value.[7,9]

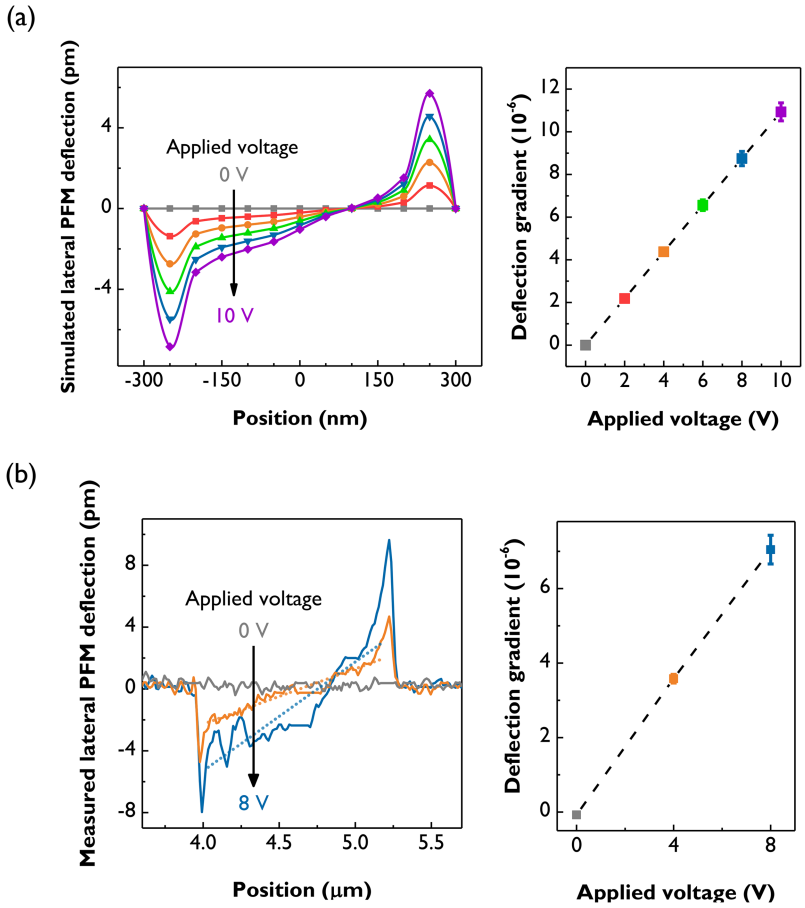

FIG. 4. (a) (i) Simulated lateral PFM signals as a function of applied voltage. (ii) The gradient of the response as measured between the peaks (the "deflection gradient") plotted as a function of the applied voltage. A linear relationship is observed, characteristic of the piezoelectric effect. (b) (i) Measured PFM signals from an individual nanowire as a function of applied voltage. (ii) The deflection gradient also displays linear dependence on the applied voltage.

In conclusion, we have demonstrated that temperature controlled template wetting is a viable production method for highly crystalline and oriented PLLA nanowires. The combination of crystallinity and orientation leads to shear piezoelectric behaviour directly confirmed using PFM observations and validated with finite element computational modelling. The model presented here is more generally applicable to PFM measurements on nanowires of other materials and allows for accurate interpretation of PFM data. Shear piezoelectricity is a known property of PLLA but has never before been conclusively demonstrated in nanostructures. In this work, we have analysed and rationalised the PFM signals collected from PLLA nanowires, demonstrating their *shear* piezoelectric behaviour at the nanoscale with an estimated $d_{14} \approx 8$ pC/N. These results ought to have significant consequences for the use of PLLA in applications requiring a sustainable and biocompatible piezoelectric polymer. Furthermore, the demonstration of shear piezoelectricity in nanostructures is an exciting prospect which has widespread implications for their use within nanogenerators, sensors, and actuators, particularly for *in vivo* biomedical applications.

Materials: Poly-L-lactic acid was purchased from Sigma Aldrich (avg. $M_n = 50\,000$). 1.4-dioxane (>99% anhydrous) was also purchased from Sigma Aldrich for use as a solvent. Whatman Anopore anodised aluminium oxide (AAO) filter membranes were used as template materials—nominal thickness and pore diameter 60 μm and 200 nm, respectively.

Characterisation: Nanowire morphology was investigated using scanning electron microscopy (Hitachi T3030). Differential scanning calorimetry was carried out using a TA instruments QA2000 DSC. Samples of between 2 and 5 mg were prepared and heated at a rate of 5 °C/min. X-ray diffraction measurements were performed using a Bruker D8 diffractometer and Cu Kα radiation. Both nanowire

powders and nanowires within the template were investigated using zero-background silicon sample holders. Piezo-response force microscopy was performed using a Bruker Multimode 8 atomic force microscope with antimony doped silicon tips (Bruker MESP-V2-RC). Samples were prepared by casting nanowire dispersions onto indium tin oxide (ITO) coated glass and fixed to AFM holders with conducting silver paint (see the supplementary material, S4).

Modelling: COMSOL Multiphysics 5.2a was used to model the nanowire deformation as a result of the field between the tip and substrate. The model calculates the steady state response of the wire, which is sufficient to accurately represent the experimental conditions, given the difference between 35 kHz applied field frequency and 0.1 Hz scan rate, i.e., at each sample point there is sufficient time for any transient response to decay. Details of the modelling including parameters used are provided in S6 of the supplementary material.

See supplementary material for details provided about the crystal phases of PLLA, fabrication, and heat treatment of nanowires used in this study, including further XRD studies. The PFM setup and calibration are described, including PFM images of nanowires, details of modelling used to interpret PFM data, and subsequent evaluation of d_{14}.

S.K.-N., Y.C., and M.S. are grateful for financial support from the European Research Council through an ERC Starting Grant (Grant No. ERC-2014-STG-639526, NANOGEN). M.S. gratefully acknowledges studentship funding from the Cambridge Commonwealth, European and International Trust. Q.J. is grateful for financial support through a Marie Sklodowska Curie Fellowship, No. H2020-MSCAIF-2015-702868. This work was partially funded by the Cambridge Synthetic Biology Strategic Research Initiative through a SynBio Fund. Supporting data for this paper is available at the DSpace@Cambridge data repository (http://dx.doi.org/10.17863/CAM.8582).

[1] E. Fukada, Ultrasonics **6**, 229 (1968).
[2] J. Telega and R. Wojnar, J. Theor. Appl. Mech. **40**, 723 (2002)
[3] J. C. Anderson and C. Eriksson, Nature **218**, 166 (1968).
[4] M. Minary-Jolandan and M.-F. Yu, ACS Nano **3**, 1859 (2009).
[5] E. Fukada, Wood Sci. Technol. **2**, 299 (1968).
[6] E. Fukada and Y. Ando, J. Polym. Sci., Part A-2 **10**, 565 (1972).
[7] E. Fukada, IEEE Trans. Electr. Insul. **27**, 813 (1992).
[8] E. Fukada, IEEE Trans. Dielectr. Electr. Insul. **13**, 1110 (2006).
[9] T. Ochiai and E. Fukada, Jpn. J. Appl. Phys., Part 1 **37**, 3374 (1998).
[10] D. Garlotta, J. Polym. Environ. **9**, 63 (2001).
[11] M. Jamshidian, E. A. Tehrany, M. Imran, M. Jacquot, and S. Desobry, Compr. Rev. Food Sci. Food Saf. **9**, 552 (2010).
[12] B. Gupta, N. Revagade, and J. Hilborn, Prog. Polym. Sci. **32**, 455 (2007).
[13] J. C. Middleton and A. J. Tipton, Biomaterials **21**, 2335 (2000).
[14] C. Ribeiro, V. Sencadas, D. M. Correia, and S. Lanceros-Méndez, Colloids Surf., B **136**, 46 (2015).
[15] X. Wang, L. Dong, H. Zhang, R. Yu, C. Pan, and Z. L. Wang, Adv. Sci. **2**, 1500169 (2015).
[16] S. Crossley, R. A. Whiter, and S. Kar-Narayan, Mater. Sci. Technol. **30**, 1613 (2014).
[17] V. Cauda, G. Canavese, and S. Stassi, J. Appl. Polym. Sci. **132**, 41667 (2015)
[18] C. S. Lovell, J. M. Fitz-Gerald, and C. Park, J. Polym. Sci., Part B: Polym. Phys. **49**, 1555 (2011).
[19] T. Furukawa and E. Fukada, J. Polym. Sci., Polym. Phys. Ed. **14**, 1979 (1976).
[20] M. Smyth, V. Poursorkhabi, A. K. Mohanty, S. Gregori, and M. Misra, J. Mater. Sci. **49**, 2430 (2014).
[21] R. Inai, M. Kotaki, and S. Ramakrishna, Nanotechnology **16**, 208 (2005).
[22] H. C. Chen, C. H. Tsai, and M. C. Yang, J. Polym. Res. **18**, 319 (2011).
[23] C. Mijangos, R. Hernández, and J. Martín, Prog. Polym. Sci. **54–55**, 148 (2016).
[24] M. Steinhart, J. H. Wendorff, and R. B. Wehrspohn, ChemPhysChem **4**, 1171 (2003).
[25] R. A. Whiter, V. Narayan, and S. Kar-Narayan, Adv. Energy Mater. **4**, 1400519 (2014).
[26] A. Datta, Y. S. Choi, E. Chalmers, C. Ou, and S. Kar-Narayan, Adv. Funct. Mater. **27**, 1604262 (2017).
[27] C. Pan, J. Luo, and J. Zhu, Nano Res. **4**, 1099 (2011).
[28] L. Zhang, C. Pan, J. Zhu, and C. Wang, Nanotechnology **16**, 2242 (2005).
[29] Y. Wu, Q. Gu, G. Ding, F. Tong, Z. Hu, and A. M. Jonas, ACS Macro Lett. **2**, 535 (2013).
[30] R. A. Whiter, Y. Calahorra, C. Ou, and S. Kar-Narayan, Macromol. Mater. Eng. **301**, 1016 (2016).
[31] Y. Tajitsu, M. Kanesaki, M. Tsukiji, K. Imoto, M. Date, and E. Fukada, Ferroelectrics **320**, 133 (2005).
[32] Y. Tajitsu, Ferroelectrics **480**, 32 (2015).
[33] S. Ito, K. Imoto, K. Takai, S. Kuroda, Y. Kamimura, T. Kataoka, N. Kawai, M. Date, E. Fukada, and Y. Tajitsu, Jpn. J. Appl. Phys., Part 1 **51**, 09LD16 (2012).
[34] M. Ando, H. Kawamura, H. Kitada, Y. Sekimoto, T. Inoue, and Y. Tajitsu, Jpn. J. Appl. Phys., Part 1 **52**, 09KD17 (2013).
[35] S. Crossley and S. Kar-Narayan, Nanotechnology **26**, 344001 (2015).
[36] T. Wang, M. Farajollahi, Y. S. Choi, I. Lin, J. E. Marshall, N. M. Thompson, S. Kar-Narayan, J. D. W. Madden, and S. K. Smoukov, Interface Focus **6**, 20160026 (2016).

[37] S. J. Lee, A. P. Arun, and K. J. Kim, Mater. Lett. **148**, 58 (2015).
[38] S. V Kalinin, B. J. Rodriguez, S. Jesse, J. Shin, A. P. Baddorf, P. Gupta, H. Jain, D. B. Williams, and A. Gruverman, Microsc. Microanal. **12**, 206 (2006).
[39] C. Harnagea, A. Pignolet, M. Alexe, and D. Hesse, Integr. Ferroelectr. **38**, 23 (2001).
[40] M. Minary-Jolandan, R. A. Bernal, I. Kuljanishvili, V. Parpoil, and H. D. Espinosa, Nano Lett. **12**, 970 (2012).
[41] H. D. Espinosa, R. A. Bernal, and M. Minary-Jolandan, Adv. Mater. **24**, 4656 (2012).
[42] Y. Calahorra, R. A. Whiter, Q. Jing, V. Narayan, and S. Kar-Narayan, APL Mater. **4**, 116106 (2016).
[43] M. Minary-Jolandan and M. F. Yu, Appl. Phys. Lett. **97**, 153127 (2010)
[44] V. Sencadas, C. Ribeiro, A. Heredia, I. K. Bdikin, A. L. Kholkin, and S. Lanceros-Mendez, Appl. Phys. A **109**, 51 (2012).
[45] D. Denning, J. Guyonnet, and B. J. Rodriguez, Int. Mater. Rev. **61**, 46 (2016).
[46] F. Peter, A. Rüdiger, R. Dittmann, R. Waser, K. Szot, B. Reichenberg, and K. Prume, Appl. Phys. Lett. **87**, 082901 (2005).
[47] F. Peter, A. Rüdiger, R. Waser, K. Szot, and B. Reichenberg, Rev. Sci. Instrum. **76**, 046101 (2005).
[48] S. Saeidlou, M. A. Huneault, H. Li, and C. B. Park, Prog. Polym. Sci. **37**, 1657 (2012).
[49] M. Cocca, M. L. Di Lorenzo, M. Malinconico, and V. Frezza, Eur. Polym. J. **47**, 1073 (2011).
[50] M. Yasuniwa, K. Sakamo, Y. Ono, and W. Kawahara, Polymer **49**, 1943 (2008).
[51] T. Kawai, N. Rahman, G. Matsuba, K. Nishida, T. Kanaya, M. Nakano, H. Okamoto, J. Kawada, A. Usuki, N. Honma, K. Nakajima, and M. Matsuda, Macromolecules **40**, 9463 (2007).
[52] J. Zhang, Y. Duan, H. Sato, H. Tsuji, I. Noda, S. Yan, and Y. Ozaki, Macromolecules **38**, 8012 (2005).
[53] S. Huang, H. Li, S. Jiang, X. Chen, and L. An, Polymer **52**, 3478 (2011).
[54] C. Ribeiro, V. Sencadas, C. M. Costa, J. L. Gómez Ribelles, and S. Lanceros-Méndez, Sci. Technol. Adv. Mater. **12**, 015001 (2011).
[55] E. A. Eliseev, A. N. Morozovska, A. V. Ievlev, N. Balke, P. Maksymovych, A. Tselev, and S. V. Kalinin, Appl. Phys. Lett. **104**, 232901 (2014).
[56] N. Balke, S. Jesse, P. Yu, B. Carmichael, S. V. Kalinin, and A. Tselev, Nanotechnology **27**, 425707 (2016).